INNOVATIVE PROCESS MODEL OF TI-6AL-4V ADDITIVE LAYER MANUFACTURING USING COLD METAL TRANSFER (CMT)

P.M. Sequeira Almeida[1*], S. Williams[1**]

[1] Welding Engineering Research Centre (WERC), Cranfield University

MK43 0AL, United Kingdom

*p.m.s.almeida@cranfield.ac.uk; **s.williams@cranfield.ac.uk

ABSTRACT

New approaches to modern manufacture have emerged from Additive Layer Manufacturing (ALM) technologies over the last 25 years. These approaches provide form, fit and function to a wide range of metallic alloys and components. Wire + Arc Additive Layer Manufacture (WAALM) has gained the interest of the research community in recent years due to its high deposition rate and efficiency (100%). The technique has been presented to the aerospace manufacturing industry as a unique low cost solution for large structural components manufacture. With this process product development time, capital investment and "Buy-to-Fly" ratios can be significantly improved. One of the greatest challenges of WAALM systems is the control algorithms needed to predict optimum welding parameters in order to achieve a specific target wall width/height requirement, and maximum deposition efficiency. This paper describes a process model for multilayer Ti-6Al-4V deposition using the Gas Metal Arc Welding based process of Cold Metal Transfer. The process model is based on a Systematic Experimental Approach carried out using a regression analysis. The mathematical relationships obtained are ready to use in future large scale "intelligent" WAALM controllers.

Keywords: Wire + Arc Additive Layer Manufacture (WAALM), Additive Layer Manufacturing (ALM), Cold Metal Transfer (CMT), Ti-6Al-4V, Buy-to-Fly, Systematic Experimental Approach (SEA), High Deposition Rate.

1. INTRODUCTION

The economical gains and environmental impact of innovative Wire + Arc Additive Layer Manufacture (WAALM) solutions over traditional manufacturing technologies for large scale manufacture, is directly dependent on the processing speeds, and therefore on the deposition rates capability. The practice becomes even more ingrained for cost effective production of high value components for aerospace industry applications, such as Ti-6Al-4V, where soaring Material Utilization Factors (MUFs) of less than 15%, normally provided by traditional forging/machining routes, need to be considered [1]. For that reason, several state of the art wire based ALM solutions are being investigated at Cranfield University in the Welding Engineering Research Centre. In the present study an out-of-chamber cold wire fed Gas Tungsten Arc Welding (GTAW) solution was utilised for the fabrication of a large structural Ti-6Al-4V component. The independent control of the wire feed speed (WFS) over the net arc power, and vice versa, resulted in a precise control over the molten pool dimensions, and the

amount of metal transferred into it. The as welded component has demonstrated the enormous potential of the GTAW based system for the manufacture of large and high quality structural components. However, while geometrical accuracy and surface finish are two of the main attributes of the former system, the main drawback is still the substantial lower deposition rate capability, when compared with a Gas Metal Arc Welding (GMAW) based process. Generally, WAALM deposition rate capabilities can go up to 1kg/h for cold wire fed GTAW, while several kilograms per hour can be achieved by utilising a GMAW based system. However poor welding conditions are in general attained and reproduced by gaseous titanium arcs. In particular Direct Current Electrode Positive (DCEP)-GMAW of titanium and titanium alloys is mainly characterized as unstable, uncontrollable and very prone to severe spattering conditions, which reduces the weld bead quality and overall process efficiency. The nature of the erratic titanium arc behaviour is caused by a dynamic cathode spot relocation mechanism observed on the active cathodic region, the molten pool.

Various approaches have been examined to overcome these problems. Recently Zhang and Li [2] proposed a modified active control to improve the robustness of the One Droplet Per Pulse (ODPP) metal transfer mechanism of titanium and titanium alloys on GMAW-P base systems. Additionally Shinn, *et al.*[3] have successfully reported a hybrid approach to confine the cathode spot relocation and suppress spatter, by utilising a low power continuous wave Nd:YAG laser beam with a minimum power of 200W and a spot diameter of 0.6mm and a GMAW-P system on Ti-6Al-4V deposition.

In the present study an innovative GMAW based solution, namely Cold Metal Transfer (CMT), has been investigated for its suitability for high deposition rate ALM of Ti-6Al-4V. CMT is a modified GMAW variant based on a controlled dip transfer mode mechanism. The process delivers excellent quality, lower thermal heat input, and nearly spatter free weld. The CMT process overcomes common difficulties encountered during conventional short circuiting GMAW such as unstable process behaviour and severe spatter formation [4]. The pioneering and key determining difference when compared with conventional GMAW is that for the first time the mechanical motion of the wire is directly incorporated into the electrical process control. The reciprocated wire feeding system is synchronized with a high speed digital control that senses the arc length, short circuiting phase and thermal input transferred to the weld [5]. When the wire moves forward and dips in the molten pool the digital control senses the voltage drop and that a short circuiting phase occurred and the current is then reduced to a significantly lower level. A feedback signal returns to the wire feeder in order to reverse the feeding direction. Then the wire back-drawing force assists the liquid bridge fracture [6] and the droplet detachment takes place. The metal transfer occurs by surface tension at near zero current. The arc ignition is initiated by an initial pulse of current that re-establishes the arc length and pre-melts a considerable amount of the wire volume. It should be noted that the movement of the motor of the driving unit is based on optimized arc characteristics rather than predefined times or speeds [7].

A key element of the successful application of WAALM is the development of a process model that enables the prediction of weld bead geometry from the process parameters. Distinct mathematical approaches have been employed for this spanning from statistical to numerical methods. Factorial designs [8, 9], linear regression [10, 11], response surface methodology [12-14], artificial neural networks (ANNs) [15, 16], taguchi method [17-21], controlled random search (CRS), or combinations of two techniques [22] have been reported. In this paper a process model for multilayer Ti-6Al-4V WAALM utilising the CMT is described. The process model is based on a comprehensive Systematic Experimental Approach (SEA) carried out using a regression analysis. Optimum welding conditions are

obtained in order to achieve a specified target effective wall width, height, and deposition rates. The preliminary mathematical relationships obtained are ready to use in future large scale "intelligent" WAALM controllers, and presently undergoing an optimization process.

2. EXPERIMENTAL

2.1 Materials

The experiments were conducted on Ti-6Al-4V substrates with dimensions 170 mm x 170 mm x 8mm. The chemical composition of the alloy (in wt. %) is provided in Table 1. The β *transus* for this composition is approximately 995ºC. Ti-6Al-4V wire diameters were 0.9 and 1.2mm spool with the chemical composition also shown in Table 1.

Table 1. Chemical composition of Ti-6Al-4V including alloying elements and impurities content (wt. %).

Alloy	Al	Mo	V	Cr	Fe	C	Si	H	N	O	Ti
Ti-6Al-4V[1]	6.28	-	4.15	-	0.15	0.03	-	0.01	0.04	0.12	Balance
Ti-6Al-4V[2]	6.14	-	3.96	-	0.18	0.02	-	0.001	0.011	0.14	Balance

[1] chemical composition for the substrate; [2] chemical composition for the 0.9 and 1.2mm wires.

2.2 Welding

Four state of the art high deposition rate WAALM systems, namely CMT, GTAW; using two variants Pulsed (GTAW-P) and Gas Tungsten Constricted Arc Welding (GTCAW); and DCEP-GMAW, were utilised during this investigation to lay down single and multilayer Ti-6Al-4V deposits. Firstly the DCEP-GMAW system was used for high deposition rate single bead on plate experiments in order to assess the welding arc stability, the quality of the deposited beads and reproducibility of the process. The same procedure was subsequently applied to the CMT system. In the latter the impact of different shielding gas mixtures on the resultant Ti-6Al-4V single bead microstructures, containing Ar/He (30%, 50% and 70%), was investigated. Additionally, a series of Ti-6Al-4V multilayer walls (10 layers), were deposited in a linear sequence utilising both the CMT and GTAW-P systems in order to assess the deposits grain size distribution and morphology, as represented schematically in Fig. 1. Finally, and for the first time the *InterPulse* GTCAW system was employed as a heat source for the fabrication of a large structural Ti-6Al-4V component, of dimensions 1000mm wide x 200mm height x 4mm thick, using an out-of-chamber technique. The welding conditions are provided in Table 2 for each individual system.

The welding torches were coupled to a pre programmed six-axis ABB industrial manipulator, in order to reproduce the welding torch transverse speeds in an accurate and repeatable sequence. An effective inert atmosphere (Ar 99.998%) was provided on–the–fly by a dedicated two inlet trailing shielding gas device, where 30L/min flow rate per inlet was used. In order to comply with a consistent build up strategy each subsequent layer was laid on top of the previous layer only when the latter had cooled down and stabilised at room temperature. An infrared pyrometer was used to monitor the substrate temperature between layers.

Table 2. CMT, GTAW-P and DCEP-GMAW welding conditions.

Process/ wire	WFS (m/min)	TS (m/min)	I_{AVG} (A)	V_{AVG} (V)	E_{ff} (η)	HI (J/mm)	Gas/Flow (l/min)	CTWD (mm)	Substrate T (ºC)	DR (kg/h)
CMT (1.2mm)	8.5	0.567	145.8	14.6	0.9	224.1	Ar-He (50%)/15	13.0	RT	2.58
DCEP-GMAW[1]	5	0.300	45.6	16.0	0.8	105.4	Ar (100%)/20	13.0	RT	0.85
DCEP-GMAW[1]	10	0.300	80.1	17.0	0.8	196.1	Ar (100%)/20	13.0	RT	1.71

WFS, wire feed speed; *TS*, travel speed; I_{AVG}, average instantaneous current; V_{AVG}, average instantaneous voltage; E_{ff} *(η)*, efficiency factor; *HI*, heat input considering an efficiency of 0.9 for CMT and 0.8 for DCEP-GMAW; *CTWD*, contact tip to work distance; *RT*, room temperature considered as approximately 25ºC; *DR*, deposition rate considering the Ti-6Al-4V ρ(kg/m^3)=4470; [1] utilising 0.9mm wire.

Table 3. GTCAW conditions.

Process/ wire	WFS (m/min)	TS (m/min)	I_p (A)	*InterPulse* I (A)	I_b (A)	t_p (s)	t_b(s)	I_{AVG} (A)	HI (J/mm)	Gas/Flow (l/min)	DR (kg/h)
GTAW-P[2]	1.6	0.270	250	-	45	0.05	0.14	98.9	158.3	Ar (100%)/20	0.49
GTCAW[2]	1.8	0.210	150	125	70	0.05	0.05	118	242.7	Ar (100%)/20	0.55

I_p, peak current*; InterPulse I*, InterPulse current; I_b, background current; t_p, pulse time; t_b, background time; *HI*, heat input considering an efficiency of 0.6 for GTAW-P and GTCAW*; CTWD*, contact tip to work distance of 3.5mm; [2] utilising 1.2mm wire.

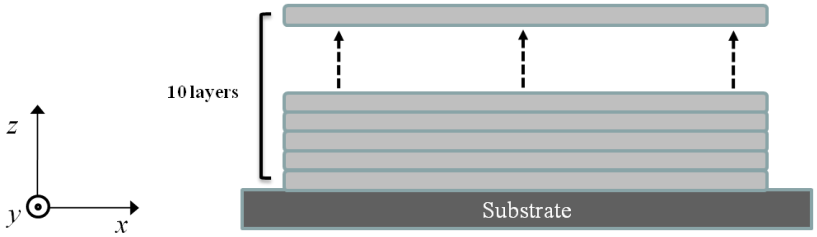

Fig. 1 WAALM multilayer procedure consisting of 10 layers of Ti-6Al-4V deposited on a substrate of the same material. The deposition direction, hence the starting point position, alternates between layers in the *–x* and *+x*.

The electrical transient data was monitored and recorded by means of a Yokogawa DL750 ScopeCorder utilising a 5 kHz acquisition rate pre-setting as standard. The Average Instantaneous Power (AIP) method (1) was employed to calculate the arc energy (W) and thereafter the heat input (2) as standard. For the GTCAW system a square current waveform was assumed and a simplistic strategy was employed to calculate the average current as given by equation (3). The welding conditions utilised in the present investigation are presented in Table 2 and Table 3.

$$AIP\,[W] = \sum_{i=1}^{n} \frac{I_i \cdot V_i}{n} \qquad (1)$$

$$HI\,[J/mm] = \eta \cdot \frac{API\,[W] \cdot 0.06}{TS\,[m/\min]} \qquad (2)$$

$$I_{AVG}\,[A] = \frac{\frac{(I_p + I_{InterPulse})}{2} + \frac{(I_b + I_{InterPulse})}{2}}{2} \quad (3)$$

The samples were mechanically sectioned and polished. They were etched in a Kroll´s solution (1% HF, 2% HNO_3, and the balance distilled H_2O) and examined using a Nikon Optiphot-66 optical microscope.

3. RESULTS AND DISCUSSION

3.1 Large structural Ti-6Al-4V components

The GTCAW power source was employed for the first time as a heat source for WAALM of a large Ti-6Al-4V structural component (Fig. 2).The GTCAW uses current converter modules to transform DC current into high frequency (20kHz) current pulses in order to produce an electromagnetic constricted arc. The high frequency current can be superimposed into a low frequency GTAW-P waveform allowing a relatively low net heat input to be delivered. The potential of GTCAW technology for Ti-6Al-4V WAALM applications is shown in Fig. 2 where a high quality large scale Ti-6Al-4V component is presented. Overall, the electromagnetic arc constriction phenomena caused by the high frequency current modulation results is believed to result in a more stable, narrower and stiffer arc plasma [23], which ultimately improves the control over the heat source. Additionally, a narrower arc column favours higher energy densities, less thermal distortion, enhancing cooling rates and therefore the heat affected zone. As demonstrated by Sundaresan, *et. al* [24] for the case of low pulsing frequency GTAW, the superior frequency pulsing capability of the *InterPulse* system, in the range of the kHz, strongly suggests a vast potential for prior-β grain refinement.

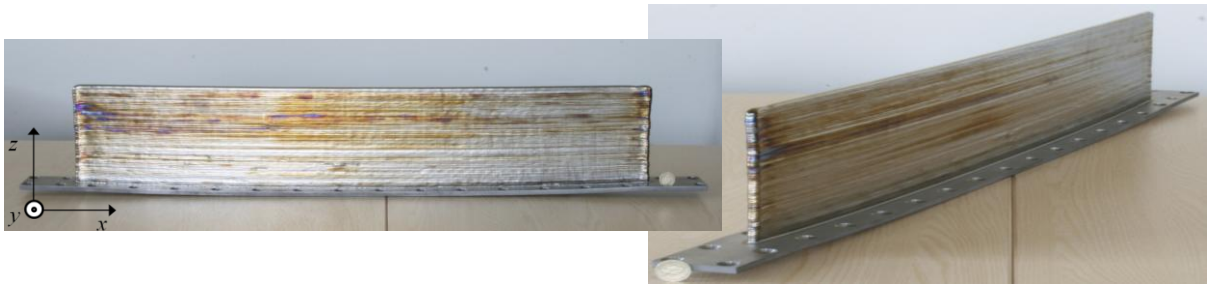

Fig. 2 WAALM large scale structural Ti-6Al-4V component of dimensions 1000mm wide x 200mm height x 4mm thick. The deposition direction, hence the starting point position, alternates between layers in the *–x* and *+x.*

As a result, optimum mechanical properties by precise control over macro and microstructures are likely to become readily available. A comprehensive mechanical testing work plan which includes tensile, fatigue and crack propagation tests, in different locations and orientations is being carried out in partnership with Bombardier.

3.2 Single bead on plate Ti-6Al-4V deposition trials by using DCEP-GMAW and CMT

Two consumable electrode GMAW solutions were investigated for high deposition rate applications of Ti-6Al-4V WAALM, DCEP-GMAW and the CMT processes. The welding conditions provided by each independent system were assessed, such as arc plasma stability, spatter level, the overall quality of the deposited beads and reproducibility of the process. As expected, and as shown in Fig. 3 very poor welding conditions were achieved with the DCEP-

GMAW system, when using low or intermediate current settings. The erratic cathode spot behaviour and very coarse spattering conditions are well illustrated in Fig. 3a for low current conditions. Even for intermediate current conditions (Fig. 3b) the gravity dominant globular transfer mechanism induces coarse spattering conditions and arc wandering.

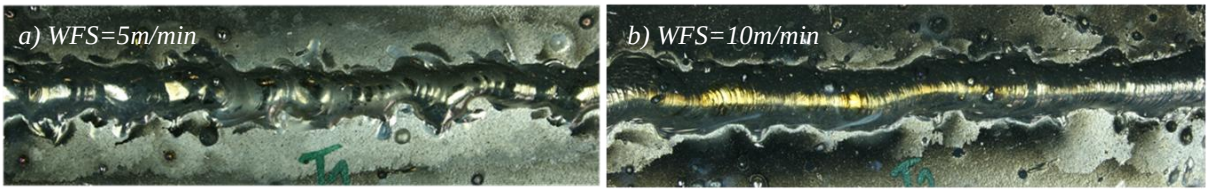

Fig. 3 Irregular bead on plate Ti-6Al-4V deposits, caused by arc wandering and coarse spattering conditions in DCEP-GMAW, here represented at different feeding rates a) WFS=5m/min and b) WFS=10m/min.

In contrast and as illustrated in Fig. 4 the CMT process has shown to prevent the cathode spot relocation mechanism during Ti-6Al-4V deposition. High quality Ti-6Al-4V welds were produced where uniform, consistent and highly reproducible results were obtained. The main reason for such difference, when compared with the DCEP-GMAW system, can be explained by the different metal transfer mechanisms. The extremely controlled dip transfer mode regime of the CMT assures that no free flight droplet is transferred during the arcing period. Thus, the repulsion of filler metal caused by the acting momentum of external electromagnetic "pinch" forces, or issuing cathode jets, on incorporated droplets is prevented. Moreover, the metal transfer to the molten pool occurs by the surface tension mechanism at low current levels, where a back-drawing force assists the liquid bridge fracture.

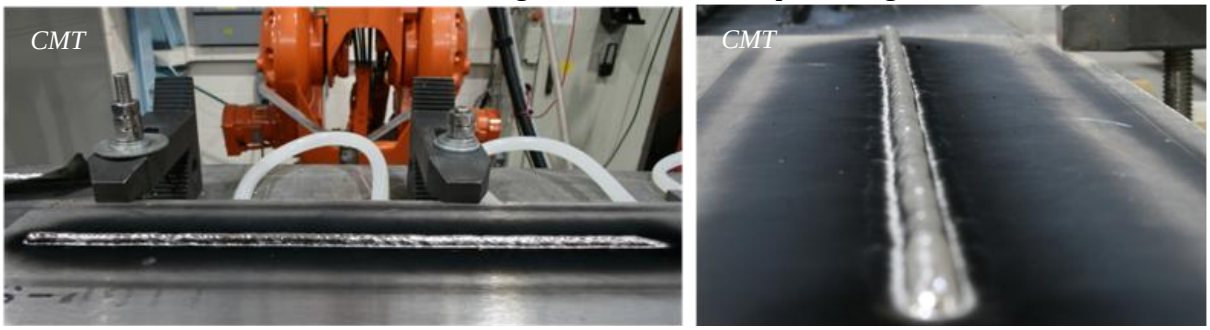

Fig. 4 CMT single bead on plate Ti-6Al-4V deposits showing that the cathode spot relocation mechanism was prevented and the spattering mechanism suppressed.

3.3 Effect of the shielding gas composition and welding multipass on Ti-6Al-4V grain size

The encouraging Ti-6Al-4V deposition results obtained from the preliminary CMT study called for an in-depth microstructural analysis. The effect of different shielding gas mixtures on the grain size dimensions and its morphology in the fusion zone was investigated. A sequence of optical macrograph results obtained from a series of single bead on plate Ti-6Al-4V trials for gas mixtures of 30%, 50% and 70% He (balance Ar) are shown in Fig. 5. Welding conditions were wire diameter 0.9 mm, WFS 12m/min and TS of 0.4 m/min. Measured heat inputs were 290, 324 and 363 J/mm for the 30%, 50% and 70% He mixtures, respectively. A higher heat input is due to the hotter arc promoted by the larger helium content. This results from the higher ionisation potential for helium compared to argon $Ar_{ionis}(V)=15.75$; $He_{ionis}(V)=24.58$. From Fig. 5 one can see that finer prior β grains are obtained by using shielding gas mixtures containing higher He content.

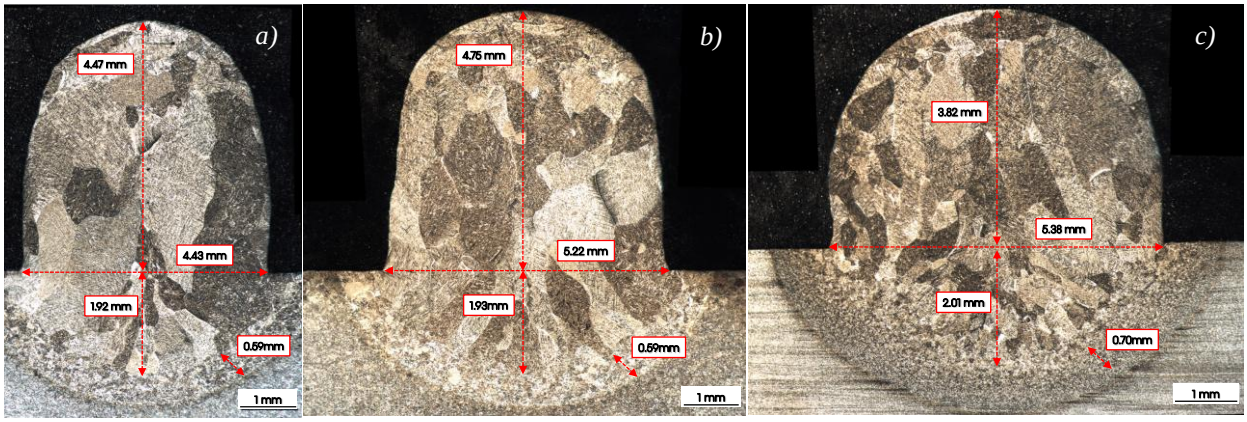

Fig. 5 Optical macrographs of CMT welds showing the effect of different shielding gases mixtures a) He(30%), b) He(50%) and c) He(70%) and the balance argon, on the grain size and its morphology in the fusion zone of single bead on plate Ti-6Al-4V deposits.

The reasons behind such prior β grain refinement effect, when utilising higher He contents in the gas shielding mixtures and therefore larger arc powers, might be attributed to a variety of different mechanisms: 1) higher T gradients promote intensive force convection and mass transport, breaking primary columnar grains near the S/L interface or promoting a globular structure by spherical growth; 2) fine solid nuclei will work as "seeds" or nucleation sites within the liquid and therefore decrease the energy barrier for heterogeneous nucleation; 3) the CMT dip transfer mechanism induces a stirring effect reducing energy barrier for homogeneous nucleation; 4) augment of the cooling rate due to the larger specific weld bead contact areas.

Following this investigation, a series of Ti-6Al-4V WAALM multilayer walls have been manufactured by using the CMT and GTAW-P system as shown schematically in Fig. 1, in order to evaluate the impact of multipass deposition, and therefore thermal field, on the grain size distribution and morphology. The results obtained for the CMT and for the GTAW-P systems are shown in Fig. 6 in the form of longitudinal cross sections, and the welding conditions indicated in Table 2 and Table 3, respectively. The GTAW-P multilayer Ti-6Al-4V macrograph is shown in Fig. 6b and exhibits a typical continuous large columnar prior β grain structure [25, 26] (1.16±0.21mm wide, CI=2σ) that emerge epitaxially from the substrate following a preferential crystallographic direction <001> across the multiple deposited layers. A relatively fine equiaxial grain structure is identified in the first deposited layer where the heat was efficiently extracted by the substrate and whereby the lower activation energy barrier against heterogeneous nucleation is easily overcome. On subsequent layers larger and less number of prior β grains are present as nucleation sites, and therefore less crystallographic directions are available. Thus, only the most rapid β grains evolving in the direction <001> will survive the growth process. Although utilising twice the arc power of the GTAW-P system as well as a larger HI, the CMT multilayer Ti-6Al-4V macrograph shown in Fig. 6a exhibits a finer grained macrostructure across the full specimen area. The epitaxial grain growth mechanism also shows a preferential vertically orientated direction <001>, however exhibiting a larger number of available nucleation sites per layer when compared with the GTAW-P macrograph revealed in Fig. 6b. Typical horizontal layer bands are observed parallel to the deposition direction in both systems as a result of the repeated thermal cycles caused by the dual solid α+β phase field region as it undergoes the transformation. The location of three layer bands as well as the thermal history (β→ α+β transformation) experienced by the 10th layer, can be seen in Fig. 6a.

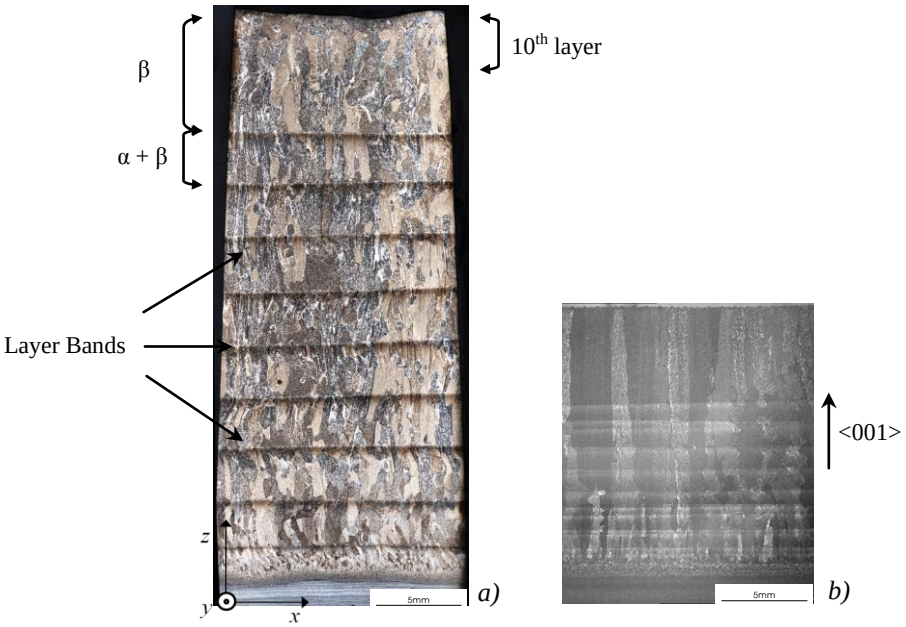

Fig. 6 Longitudinal cross sections of WAALM of Ti-6Al-4V multilayer deposits showing the epitaxial prior β grains developments and layer band morphology for the a) CMT and b) GTAW-P welding processes. The thermal history experienced by the 10th layer **(**β→ α+β**)** is schematically represented for the CMT as well as the crystallographic direction <001>.

3.4 Process Model of CMT Ti-6Al-4V WAALM

The success of "intelligent" and fully automated WAALM systems is strongly dependent on accurate predictions of the optimum welding process parameters in order to achieve a target weld bead geometry, and vice versa. The bead geometry requisite is to be specified by a Computer Aided Design (CAD) solid model and should comprise the effective wall width as well as the step increment dimension per deposited layer, hence the bead height output. In this section an empirical process model based on discrete experimental results for multilayer Ti-6Al-4V deposition using the GMAW based process of Cold Metal Transfer is described. A comprehensive SEA strategy was adopted utilising three controllable factors and several other responses. The controllable variables included the solid wire diameter, WFS and WFS/TS ratios. Ti-6Al-4V 0.9 and 1.2mm wire diameters were used and the WFS settings for each individual wire ranged from 2 to 12m/min, in a unit basis. The WFS/TS ratios were 15, 20 and 25. It should be noted that the WFS/TS ratio has been selected as an independent factor – rather than TS – guaranteeing good welding conditions and high quality deposits all over the design space. Data was fed into a least squares regression analysis software and the main effects and interactions between controllable variables and responses were estimated. Several responses were selected and measured, although only the effective wall width and the deposition efficiency are reported here. The effective wall width is defined in the present context as the target wall width dimension, after undergoing the post processing machining stage. On the other hand the deposition efficiency estimates the ratio between the effective volume of metal utilised to net shape the component over the total delivered metal volume. A typical first order 3D response surface output, namely the effective wall width, is represented in Fig. 7 as a function of the wire diameter and the WFS, for constant WFS/TS of 20. It can be seen that larger effective wall widths are achieved with thicker wires for constant WFS and WFS/TS ratio.

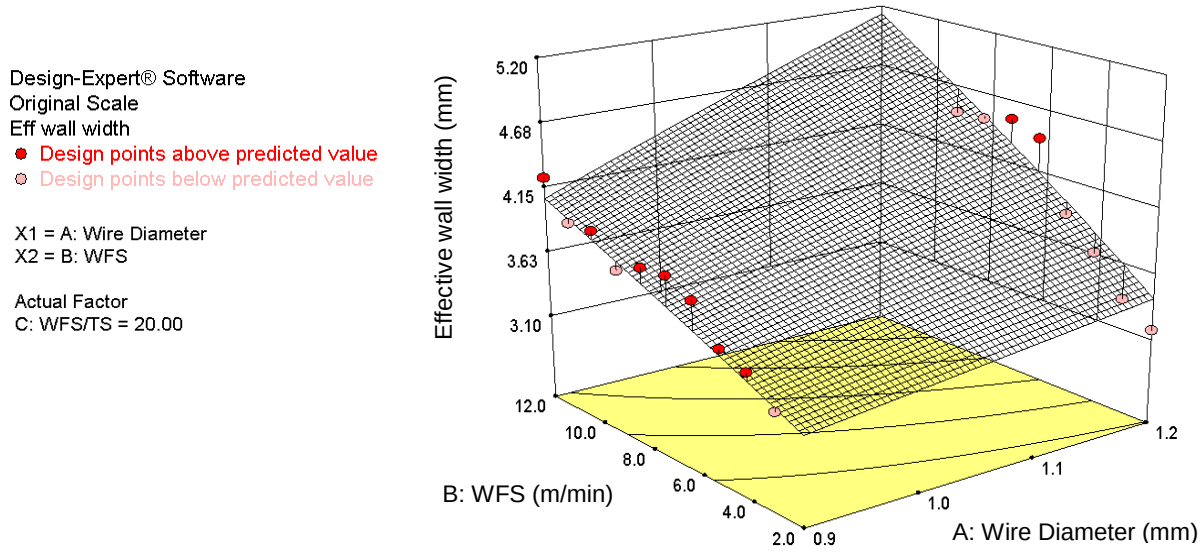

Fig. 7 Predicted first order 3D response surface model for the effective wall width response as a function of the wire diameter and the WFS, for constant WFS/TS ratio of 20.

In order to maximize the confidence level on the attained regression model a series of *adequacy checking* steps were undertaken throughout the *Analysis of Variance (ANOVA).* The residuals[3] diagnostic procedure was successfully undertaken and a structureless pattern trend has been observed. The best power transformation was also recommended and employed λ=1.63 in order to improve the new residual sum of squares (SS) output. Moreover, the obtained Adjusted R^2=0.896 and the Prediction R^2=0.874 terms were acceptable and considered essential to support how good the model predictions are likely to be. As expected higher correlation values are desired in order to maximize the confidence level of the model predictions. Additionally, the Adjusted R^2 and Prediction R^2 terms have shown to be within 0.20 of each other, and therefore in very good agreement. Finally, a considerable signal-to-noise ratio value was obtained (F-value=87.16), whereas non significant effects were ignored using a default level of significance threshold p-value<0.1 (confidence interval of 90%), indicative that the individual term has a high level of significance on the response. Overall, accurate predictions involve reasonable consistency and stable variance during the process model development.

Measured deposition efficiencies for single 1.2mm Ti-6Al-4V wires are plotted in Fig. 8 as a function of the target effective wall width. It is seen that effective wall widths ranging from 3.2 to 5.2mm were achieved with deposition efficiencies over 80%. As expected, it is also observed that effective wall widths are dependent on the WFS/TS ratio.

[3] The *n* deviations between the sample and either, the (observed) *sample* average or the regressed (fitted) function value. These residuals always sum to zero $\sum(y_i - y_{avg}) = 0;\ i = 1,2,\dots,n$; establishing a linear constrain. [27]

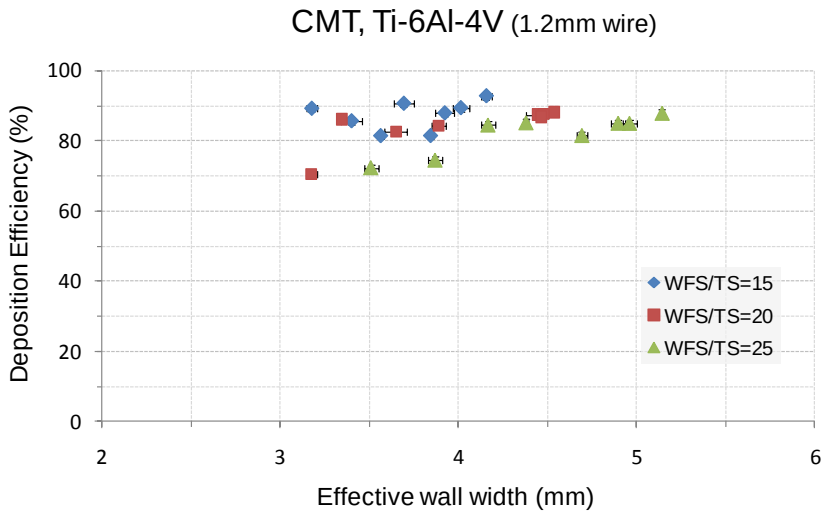

Fig. 8 Measured deposition efficiencies as a function of the target effective wall width for CMT Ti-6-Al-4V multilayer deposition for different cross section deposited areas (WFS/TS).

4. CONCLUSIONS

A state of the art GTAW solution, Gas Tungsten Constricted Arc Welding (GTCAW), has been utilised for the first time for Ti-6Al-4V WAALM of a high quality large structural component in an out of chamber environment. The electromagnetic arc constriction phenomena, as well as the independent control of the wire feed speed and current, favoured the overall control over the arc heating source, heat input, thermal distortion and metal transfer during layer upon layer deposition process.

The innovative Cold Metal Transfer (CMT) GMAW variant overcomes common deposition issues related with titanium arcs, such as arc wandering and severe spattering conditions, providing high quality and spatter free deposits with low heat input and excellent reproducibility. CMT has demonstrated to be a high deposition rate ALM solution for large scale manufacture of Ti-6Al-4V structural components. It was also shown that grain size dimensions and its morphology in the fusion zone, in CMT single bead on plate welds, is dependent on the shielding gas composition. Finer prior β grains were obtained by using shielding gas mixtures with higher He content. In the case of Ti-6Al-4V multipass deposition, and although utilising larger energy inputs, the CMT process had a much refined prior β grain growth when compared with the continuous large columnar prior β grain structure provided by the GTAW-P system. In both cases a preferential vertically orientated grain growth direction <001> is identified, though in the case of the CMT, with a large number of nucleation sites and crystallographic directions available.

A process model has been developed for the CMT process of Ti-6Al-4V deposition for WAALM utilising the least squares regression analysis method. This model enables the determination of process parameters for specific target wall width sizes. The effective wall width response was modelled and has shown to be in good agreement with the empirical data. For 1.2mm Ti-6Al-4V wires effective wall widths range from 3.2 to 5.2mm wide with deposition efficiencies over 80% and deposition rates in excess of 3kg/hr.

AKNOWLEDGMENTS

The present work was developed within the Ready to Use Additive Manufacture (RUAM) framework and financially supported by the Engineering and Physical Sciences Research Council (EPSRC) via the Innovative Manufacturing Research Centre (IMRC) at Cranfield University, and AIRBUS, under the project number 131.

1. Witt, R.H. and A.L. Ferreri, *Titanium near net shape components for demanding airframe applications.* S.A.M.P.E. quarterly, 1986. **17**(3): p. 55-62.

2. Zhang, Y.M. and P.J. Li, *Modified active control of metal transfer and pulsed GMAW of titanium.* Welding Journal (Miami, Fla), 2001. **80**(2): p. 54-S.

3. Shinn, B.W., D.F. Farson, and P.E. Denney, *Laser stabilisation of arc cathode spots in titanium welding.* Science and Technology of Welding and Joining, 2005. **10**(4): p. 475-481.

4. Hermans, M.J.M. and G.D. Ouden, *Process Behaviour and Stability in Short Circuit Gas Metal Arc Welding.* Welding Journal (Miami, Fla), 1999. **78**(4): p. 137-141-s.

5. Pickin, C.G. and K. Young, *Evaluation of cold metal transfer (CMT) process for welding aluminium alloy.* Science and Technology of Welding and Joining, 2006. **11**(5): p. 583-585.

6. Feng, J., H. Zhang, and P. He, *The CMT short-circuiting metal transfer process and its use in thin aluminium sheets welding.* Materials and Design, 2009. **30**(5): p. 1850-1852.

7. Lorenzin, G. and G. Rutili, *The innovative use of low heat input in welding: Experiences on 'cladding' and brazing using the CMT process.* Welding International, 2009. **23**(8): p. 622-632.

8. Raveendra, J. and R.S. Parmar, *Mathematical models to predict weld bead geometry for flux cored arc welding.* Metal construction, 1987. **19**(1).

9. Sivagami, S.M. and N. Murugan, *Development of mathematical models for prediction of weld bead geometry of hardfaced gate valve by plasma transferred arc surfacing.* Welding in the World, 2009. **53**(SPECIAL ISSUE): p. 393-398.

10. Yang, L.J., M.J. Bibby, and R.S. Chandel, *Linear regression equations for modelling the submerged-arc welding process.* Journal of Materials Processing Tech., 1993. **39**(1-2): p. 33-42.

11. Yang, L.J., R.S. Chandel, and M.J. Bibby, *The Effect of Process Variables on the Weld Deposit Area of Submerged Arc Welds* Welding Journal, 1993. **72**(1): p. 11-s to 18-s.

12. Kim, D., S. Rhee, and H. Park, *Modelling and optimization of a GMA welding process by genetic algorithm and response surface methodology.* International Journal of Production Research, 2002. **40**(7): p. 1699-1711.

13. Gunaraj, V. and N. Murugan, *Prediction and optimization of weld bead volume for the submerged arc process - Part 1.* Welding Journal (Miami, Fla), 2000. **79**(10).

14. Gunaraj, V. and N. Murugan, *Application of response surface methodology for predicting weld bead quality in submerged arc welding of pipes.* Journal of Materials Processing Technology, 1999. **88**(1): p. 266-275.

15. Andersen, K., et al., *Artificial neural networks applied to arc welding process modelling and control.* IEEE Transactions on Industry Applications, 1990. **26**(5): p. 824-830.

16. Nagesh, D.S. and G.L. Datta, *Prediction of weld bead geometry and penetration in shielded metal-arc welding using artificial neural networks.* Journal of Materials Processing Technology, 2002. **123**(2): p. 303-312.

17. Murugan, N. and R.S. Parmar, *Effects of MIG process parameters on the geometry of the bead in the automatic surfacing of stainless steel.* Journal of Materials Processing Tech., 1994. **41**(4): p. 381-398.

18. Rao, P.S., et al., *Effect of process parameters and mathematical model for the prediction of bead geometry in pulsed GMA welding.* International Journal of Advanced Manufacturing Technology, 2009. **45**(5-6): p. 496-505.

19. Tarng, Y.S. and W.H. Yang, *Optimisation of the weld bead geometry in gas tungsten arc welding by the taguchi method.* International Journal of Advanced Manufacturing Technology, 1998. **14**(8): p. 549-554.

20. Murugan, N., R.S. Parmar, and S.K. Sud, *Effect of submerged arc process variables on dilution and bead geometry in single wire surfacing.* Journal of Materials Processing Tech., 1993. **37**(1-4): p. 767-780.

21. Tarng, Y.S., S.C. Juang, and C.H. Chang, *The use of grey-based Taguchi methods to determine submerged arc welding process parameters in hardfacing.* Journal of Materials Processing Technology, 2002. **128**(1-3): p. 1-6.

22. Tarng, Y.S., W.H. Yang, and S.C. Juang, *Use of fuzzy logic in the Taguchi method for the optimization of the submerged arc welding process.* International Journal of Advanced Manufacturing Technology, 2000. **16**(9): p. 688-694.

23. Onuki, J., et al., *Development of a new high-frequency, high-peak current power source for high constricted arc formation.* Japanese Journal of Applied Physics, Part 1: Regular Papers and Short Notes and Review Papers, 2002. **41**(9): p. 5821-5826.

24. Sundaresan, S., G.D. Janaki Ram, and G. Madhusudhan Reddy, *Microstructural refinement of weld fusion zones in α-β titanium alloys using pulsed current welding.* Materials Science and Engineering A, 1999. **262**(1-2): p. 88-100.

25. Baufeld, B., O.V.D. Biest, and R. Gault, *Additive manufacturing of Ti-6Al-4V components by shaped metal deposition: Microstructure and mechanical properties.* Materials and Design. **31**(SUPPL. 1).

26. Brandl, E., et al., *Deposition of Ti-6Al-4V using Nd:YAG laser & wire: Microstructure and mechanical properties*, in *NATO AVT-163 Specialists Meeting on Additive Technology For Repair of Military Hardware*. 2009: Bonn.

27. Box, G.E.P., J.S. Hunter, and W.G. Hunter, *Statistics for experimenters : design, innovation, and discovery*. 2nd ed. ed. Wiley series in probability and statistics. 2005, Hoboken, N.J.: Wiley. xvii, 633 p.